

# Structural Characterization of 4-Cyanoimidazolium-5-olate, 4,4-Diphenyl-5-imidazolinone, and 4,5-Dicyanoimidazole. A Novel Mesoionic Compound and Decoding of Intermolecular Hydrogen Bonds

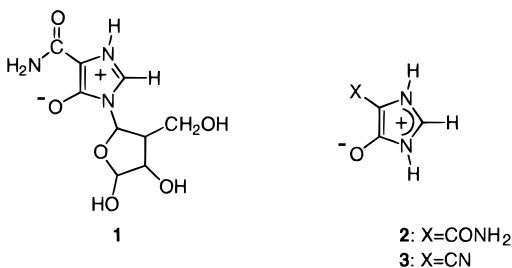
Ermanno Barni,<sup>†</sup> Riccardo Bianchi,<sup>‡</sup>  
Giuliana Gervasio,<sup>\*§</sup> Arnold T. Peters,<sup>‡</sup>  
Guido Viscardi<sup>\*†</sup>

Dipartimento di Chimica Generale ed Organica Applicata, Corso Massimo D'Azeglio 48, I-10125 Torino, Italy, Centro CNR per lo studio delle Relazioni tra Struttura e Reattività Chimica, via Golgi 19, I-20133 Milano, Italy, Dipartimento di Chimica Inorganica, Chimica Fisica e Chimica dei Materiali, via Pietro Giuria 7, I-10125 Torino, Italy, and Chemistry and Chemical Technology, University of Bradford, Bradford BD7 1DP, UK

Received November 18, 1996 (Revised Manuscript Received July 10, 1997)

## Introduction

In the field of nonlinear optics, for an organic material to be useful as a single crystal for second-order phenomena, it has to comply with several requirements:<sup>1</sup> (i) high molecular polarization to provide an optimum efficiency, (ii) noncentrosymmetry of the crystal to provide a crystalline susceptibility  $\chi^{(2)} \neq 0$ , (iii) high thermal and chemical stability to provide stability during use, (iv) for second harmonic generation, transparency properties in the visible region to eliminate autoabsorption phenomena, and (v) ease of synthesis and crystal growth. In the course of an extensive screening on imidazole derivatives as single crystals for nonlinear optics, mesoionic structures<sup>2</sup> attracted our attention owing to their molecular polarization. Some mesoionic structures for 5(4)-substituted imidazol-4(5)-ones have been reported and 1,3-diazolium-4-olates are of particular note. Bredinin (**1**)



shows immunosuppressive properties<sup>3</sup> while, its aglycon derivative **2** shows antitumor activity against sarcoma 180 and Ehrlich carcinoma and cytotoxic properties against L5178Y cells.<sup>4,5</sup> The mesoionic nature of these compounds was established by X-ray analysis.<sup>6</sup>

<sup>†</sup> Dipartimento di Chimica Generale ed Organica Applicata. Tel: +11-6707598. Fax: +11-6707591. E-mail: viscardi@silver.ch.unito.it.  
<sup>‡</sup> Centro CNR per lo studio delle Relazioni tra Struttura e Reattività Chimica.

<sup>§</sup> Dipartimento di Chimica Inorganica, Chimica Fisica e Chimica dei Materiali. Tel: +11-6707504. Fax: +11 6707855. E-mail: gervasio@silver.ch.unito.it

<sup>1</sup> University of Bradford.

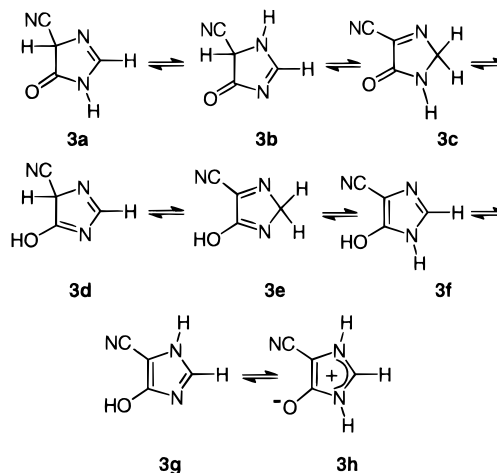
(1) Nicoud J. F.; Twieg R. J. *Nonlinear Properties of Organic Molecules and Crystals*; Chmela, D. S., Zyss, J., Eds.; Academic Press: New York, 1987; Vol. 1, p 227.

(2) Ramsden C. A. *Comprehensive Organic Chemistry*, Barton, D. H. R., Ollis, W. D., Eds.; Pergamon Press: Oxford, 1979; Vol. 4, p. 1171.

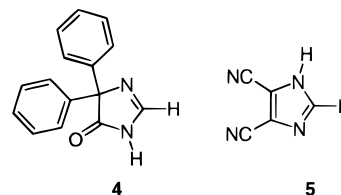
(3) Hayashi, M.; Hirano, T.; Yaso, M.; Mizuno, K.; Ueda, T. *Chem. Pharm. Bull.* **1975**, *23*, 244.

(4) Mizuno, K.; Tsujino, M.; Takada, M.; Hayashi, M.; Atsami, K.; Asano, K.; Matsuda, T. *J. Antibiot.*, **1974**, *27*, 775.

4-Cyanoimidazolium-5-olate (**3**) showed cytostatic and anticancer activity, e.g. against sarcoma-180 and Lewis lung carcinoma P-388.<sup>7a,b</sup> We have recently used compound **3** as a coupling agent for the synthesis of heterocyclic azo dyes<sup>8</sup> and we have undertaken a structural analysis using X-ray, IR, and NMR techniques, as a contribution for understanding relationships between structures and biological and nonlinear optical properties. Compound **3** is a 5(4)-substituted imidazol-4(5)-one and therefore can exist in the eight different tautomeric forms **3a–h** because of both annular and keto–enol tautomer-



ism.<sup>9</sup> 4,4-Diphenyl-4*H*-imidazol-5-one (**4**) and 4,5-dicyanoimidazole (**5**) were also studied as models of an oxo-



tautomeric structure, in particular for the unconjugated form **3a**, and for an imidazole free from keto–enol tautomerism. The three heterocycles show also some interesting patterns of hydrogen bonds and an analysis of the hydrogen-bonding (HB) motifs was therefore undertaken.

## Results and Discussion

### Synthesis of 4-Cyanoimidazolium-5-olate (**3**).

Three synthetic pathways to compound **3** are available: (i) treatment of a mixture of the tris(trimethylsilyl) derivative of compound **2** with SOCl<sub>2</sub>, MeOH, and NEt<sub>3</sub> in THF;<sup>7a</sup> (ii) initial conversion of the carbamoyl derivative (compound **2**) to the thiocarbamoyl derivative by P<sub>4</sub>S<sub>10</sub>, followed by treatment with HgCl<sub>2</sub> in EtOH (95%) and

(5) Yoshida, N.; Kiyohara, T.; Ogino, S. 1978, G.P. 2,740,281; *Chem. Abstr.* **1978**, *89*, 488900.

(6) Yoshioka, H.; Nakatsu, K. *Tetrahedron Lett.* **1975**, *46*, 4031.

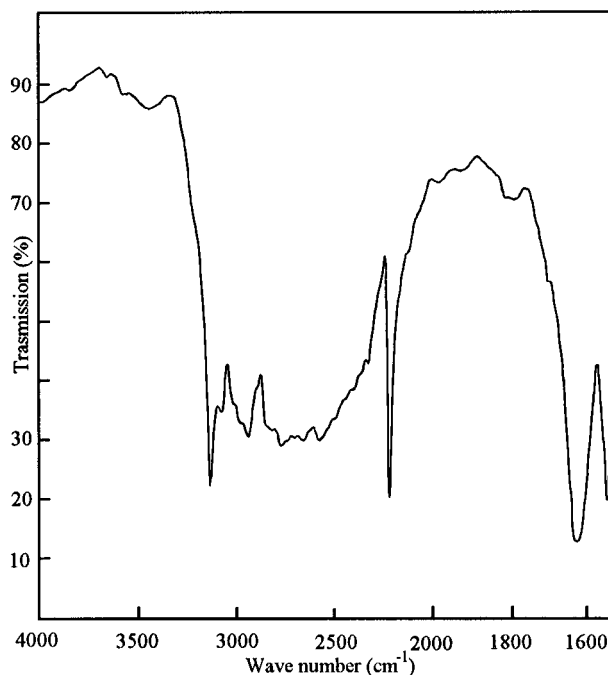
(7) (a) Sumitomo Chemical Co. 1982, JP 64,678; *Chem. Abstr.* **1982**, *97*, 110012. (b) Bakulev, V. A.; Mokrushin, V. S.; Polishchuk, N. V.; Zhuravleva, I. A.; Anoshina, G. M.; Zubova, T. E.; Pushkareva, Z. V. *Khim. Farm. Zh.* **1981**, *15*, 58; *Chem. Abstr.* **1982**, *97*, 110012r.

(8) Peters, A. T.; Wu, C. T.; Viscardi, G.; Barni, E. *Dyes Pigments* **1995**, *29*, 103.

(9) Elguero, J.; Marzin, C.; Katritzky, A. R.; Linda, P. *The Tautomerism of Heterocycles. Advances in Heterocyclic Chemistry. Supplement 1*; Katritzky, A. R.; Boulton, A. J., Eds.; Academic Press: London, 1976; p 373.

**Table 1. Molecular Characteristics from IR and NMR Data**

characteristics		conclusions
	IR	
3200–2300 cm <sup>-1</sup> (NH stretching) region $\Delta\nu_{\text{NH}} = 800 \text{ cm}^{-1}$ absence of OH stretching at 3400 cm <sup>-1</sup> stretching CO at 1625 cm <sup>-1</sup>		discounting of structures <b>3c</b> and <b>3d</b> NH group involved in hydrogen bonds discounting of structures <b>3d–g</b> discounting of structures <b>3a–c</b> suggestion of mesoionic structure <b>3h</b>
	NMR	
similarity of DMSO- <i>d</i> <sub>6</sub> and solid state <sup>13</sup> C NMR sole doublet at 131.52 ppm C(CO) at 159.62 ppm C(CN) at 115.05 ppm		prevalence of the same tautomer discounting of structures <b>3a–e</b> discounting of structures <b>3a–c</b> small contribution of structure <b>3i</b>

**Figure 1.** 4000–1550 cm<sup>-1</sup> region of the IR spectrum of compound **3** on a KBr plate.

20% aqueous MeNH<sub>2</sub>;<sup>7b</sup> and (iii) nitrosation of 2-cyano-*N*-formylacetamide and reduction of the hydroxyimino group by sodium dithionite, thus providing a one-step ring closure sequence.<sup>10</sup> The last method is the most convenient and affords satisfactory yields. Compound **3** is sparingly soluble in organic solvents and is purified by crystallization from water. DSC analysis showed no melting point but thermal degradation in the range 297–305 °C.

**IR and NMR Spectra.** IR and NMR techniques suggested the preliminary considerations reported in Table 1. The IR spectrum in KBr (4000–1550 cm<sup>-1</sup> region in Figure 1) of compound **3** showed the CH stretching at 3120 cm<sup>-1</sup>, while the remaining complex absorption in the 3200–2300 cm<sup>-1</sup> region may be ascribed to the NH group.<sup>11</sup> The bands may be due to Fermi resonance of  $\nu_{\text{NH}}$  with the in-plane,  $\delta_{\text{NH}}$ , and out-of-plane,  $\gamma_{\text{NH}}$ , bending modes, i.e.  $2\delta_{\text{NH}}$  and  $2\gamma_{\text{NH}}$ , while the minima may represent the overtone frequencies.<sup>12</sup> The presence of this NH characteristic absorption and the absence of absorption at higher wavenumbers (OH stretching at 3400 cm<sup>-1</sup>) allow us to discount structures **3d–g**. In

accordance with Bellocq et al.<sup>11</sup> and Emsley,<sup>12</sup> the shift from the nonhydrogen-bonding signal (3518 cm<sup>-1</sup>) is proposed as a parameter to estimate the intensity of a hydrogen bond. By adopting the center of absorption as the fundamental frequency of  $\nu_{\text{NH}}$ ,<sup>11</sup> a value  $\Delta\nu_{\text{NH}} = 800 \text{ cm}^{-1}$  is obtained for compound **3**. Consequently, the hydrogen bond (N–H···O, as evidenced from X-ray data) in compound **3** is stronger than that in imidazole (N–H···N,  $\Delta\nu_{\text{NH}} = 700 \text{ cm}^{-1}$ ).<sup>11</sup>

The CN stretching is detectable at 2220 cm<sup>-1</sup>, slightly shifted to lower wavenumbers than the corresponding signal of compound **5** (2260 cm<sup>-1</sup>), thus indicating a slight nonequivalence of the nitrile group in the two heterocycles. The large and intense signal at 1625 cm<sup>-1</sup> may be assigned to the stretching of the carbon–oxygen bond. In the IR spectrum (KBr) of compound **4** the carbonyl absorbs at 1725 cm<sup>-1</sup>, in agreement with data reported by Schipper et al.,<sup>13</sup> who assigned to compound **4** the unconjugated structure; the corresponding value for the conjugated tautomer is expected at 1710–1725 cm<sup>-1</sup>.<sup>13,14</sup> The comparison of the absorption at 1625 cm<sup>-1</sup> of compound **3** with the C=O stretching of compound **4** discounts structures **3a–c** and sustains the mesoionic structure **3h** in the solid state, in accordance with data reported for the oxazol-5-ones.<sup>15</sup>

The <sup>13</sup>C NMR spectra of compound **3** in the solid state (67.8 MHz) and in DMSO-*d*<sub>6</sub> solution (100 MHz) appeared very similar, suggesting that the tautomer inherent in the solid state also predominates in DMSO-*d*<sub>6</sub> and allows us to extrapolate to crystals the interesting considerations pointed out for DMSO-*d*<sub>6</sub> solution in the coupled <sup>13</sup>C NMR spectrum: (i) the doublet at 131.52 ppm, showing <sup>1</sup>J<sub>CH</sub> = 214 Hz, corresponds to the sole carbon C(2) in the ring bearing just one hydrogen, H(2), which gives a singlet at 7.70 ppm; this enables us to exclude the contribution of forms **3a**, **3b**, and **3d** (which would show two doublets) and forms **3c** and **3e** (which would show one triplet); (ii) the downfield signal (159.62 ppm) can be assigned to the carbon atom linked to oxygen and the comparison with the chemical shift of C(C=O) of compound **4** (183.71 ppm) sustains the absence of the oxo structures **3a–c**. NMR spectroscopy does not distinguish between structures **3f**, **3g**, and **3h**, but IR data suggested the prevalence of structure **3h**, so if this hypothesis is correct, the spectrum in DMSO-*d*<sub>6</sub> gives further information on the negative charge distribution. In fact, the small difference between <sup>13</sup>C signals of cyano groups of compounds **3** and **5**, at 115.05 and 111.20 ppm respectively, suggests a small contribution of the resonance structure **3i**, in agreement with the weak charge demand

(10) Cusak, N. J.; Shaw, G.; Logemann, F. I. *J. Chem. Soc. Perkin Trans. 1* **1980**, 2316.

(11) Bellocq, A. M.; Perchard, C.; Novak, A.; Josien, M. L. *J. Chim. Phys.* **1965**, *62*, 1334.

(12) Emsley, J. *J. Chem. Soc. Rev.* **1980**, 9, 91.

(13) Schipper, E.; Chinery, E. *J. Org. Chem.* **1961**, *26*, 4480.

(14) Edward, J. T.; Lantos, I. *J. Heterocycl. Chem.* **1972**, *9*, 363.

(15) Gotthardt, H.; Huisgen, R. *J. Am. Chem. Soc.* **1970**, *92*, 4340.

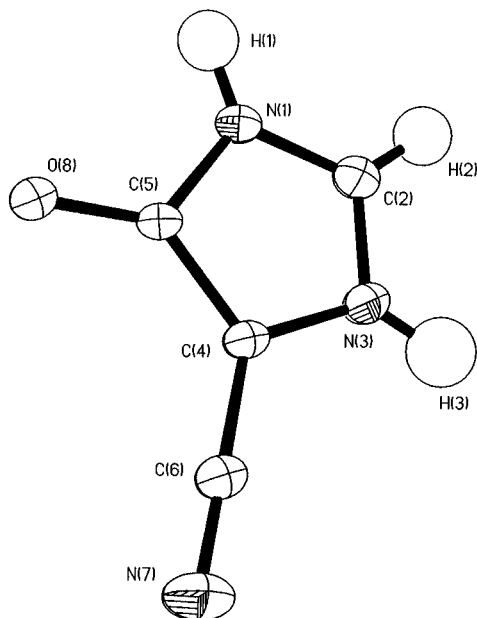
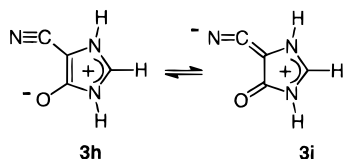


**Figure 2.** ORTEP plot (50% probability) of compound **3**, nearly perpendicular to the molecular plane.

by the cyano group observed by Pagani et al.<sup>16</sup> on carbanions of  $\alpha$ -activated acetonitriles and phenylacetone nitriles.



Finally, the signal at 80.60 ppm can be assigned to remaining carbon bearing the cyano group.

**Molecular Structure of 4-Cyanoimidazolium-5-olate (3) (C<sub>4</sub>H<sub>3</sub>N<sub>3</sub>O).** This compound crystallizes as light-yellow prisms in the orthorhombic space group *Pna*2<sub>1</sub> with  $a = 12.534(3)$  Å,  $b = 9.692(2)$  Å,  $c = 3.763(2)$  Å,  $V = 457.18(15)$  Å<sup>3</sup>,  $Z = 4$ ,  $D_c = 1.5585$  g cm<sup>-3</sup>,  $W = 109.1$ ,  $R = 0.034$  for 722 unique observed reflections with  $F > 4.0\sigma(F)$ , GOF = 0.95. Figure 2 shows the molecular structure. The more relevant and unexpected feature is the presence of the hydrogen atoms bonded to N(1) and N(3) atoms, giving rise consequently to a mesoionic structure. The bond lengths (Table 2) show a  $\pi$  delocalization in the ring involving also the substituents, and their values are in keeping with the values reported for imidazole.<sup>17</sup> The electronic delocalization has, however, various degrees of magnitude; comparing, for example, the C–N distances within the ring, it is clear that N(1)–C(2) (1.339(2) Å) and C(2)–N(3) (1.318(2) Å) bonds have a greater double bond character with respect to N(1)–C(5) (1.396(2) Å) and N(3)–C(4) (1.391(2) Å) bonds, with a prevalence of a double bond character (difference of  $9\sigma$ ) on C(2)–N(3). The C(4)–C(5) bond (1.396(2) Å) shows a smaller double bond character with respect to the corresponding bond in imidazole.<sup>17</sup> This agrees with a partial double bond character of the C(5)–O(8) bond (1.262(2) Å), which exhibits a bond order comparable with

**Table 2.** Heterocyclic Bond Lengths (Å)<sup>a</sup>

	3	4	5
N(1)–H(1)	0.91(2)	0.95(3)	0.90(2)
N(1)–C(2)	1.339(2)	1.381(3)	1.349(1)
N(1)–C(5)	1.396(2)	1.358(3)	1.364(1)
C(2)–H(2)	1.00(2)	0.92(3)	0.97(2)
C(2)–N(3)	1.318(2)	1.269(3)	1.320(1)
N(3)–C(4)	1.391(2)	1.479(3)	1.368(1)
N(3)–H(3)	0.93(2)		
C(4)–C(5)	1.396(2)	1.532(3)	1.375(1)
C(4)–C(6)	1.402(2)		
C(4)–C(7)		1.525(3)	
C(4)–C(7)		1.527(3)	
C(5)–O(6)		1.218(3)	
C(5)–O(8)	1.262(2)		
C(4)–C(8)			1.417(2)
C(6)–N(7)	1.143(2)		1.143(2)
C(5)–C(6)			1.417(1)
C(8)–N(9)			1.137(2)

<sup>a</sup> The bond lengths of benzene rings of compound **4** are reported in the Supporting Information.

**Table 3.** Heterocyclic Bond Angles (deg)<sup>a</sup>

	3	4	5
H(1)–N(1)–C(2)	126.1(16)	129.8(15)	124.0(10)
H(1)–N(1)–C(5)	123.7(15)	121.8(15)	129.0(10)
C(2)–N(1)–C(5)	110.2(1)	108.4(2)	107.0(1)
N(1)–C(2)–H(2)	127.4(12)	120.1(17)	122.0(9)
N(1)–C(2)–N(3)	109.3(2)	116.3(2)	112.7(1)
H(2)–C(2)–N(3)	123.2(12)	123.5(17)	125.3(9)
C(2)–N(3)–C(4)	108.4(1)	105.9(2)	104.2(1)
C(2)–N(3)–H(3)	119.3(17)		
C(4)–N(3)–H(3)	132.3(16)		
N(3)–C(4)–C(5)	108.2(1)	104.3(2)	110.8(1)
N(3)–C(4)–C(6)	123.2(1)		
N(3)–C(4)–C(8)			123.3(1)
C(5)–C(4)–C(6)	128.5(2)		
C(5)–C(4)–C(8)			125.9(1)
N(3)–C(4)–C(6)	123.2(1)		
C(5)–C(4)–C(6)	128.5(2)		
C(4)–C(6)–N(7)	179.4(2)		
N(1)–C(5)–C(4)	103.9(1)	105.0(2)	105.3(1)
N(1)–C(5)–C(6)			126.2(1)
N(1)–C(5)–O(8)	124.1(1)		
C(4)–C(5)–O(8)	132.0(1)		
C(4)–C(5)–C(6)			128.5(1)
C(5)–C(6)–N(7)			174.8(1)
C(4)–C(8)–N(9)			178.0(1)
N(3)–C(4)–C(7)		111.0(1)	
C(5)–C(4)–C(7)		107.3(1)	
N(3)–C(4)–C(7)		109.4(1)	
C(5)–C(4)–C(7)		112.2(1)	
N(1)–C(5)–O(6)		126.3(2)	
C(4)–C(5)–O(6)		128.7(2)	
C(7)–C(4)–C(7)		112.4(2)	

<sup>a</sup> The bond angles of benzene rings of compound **4** are reported in the Supporting Information.

the delocalized double bonds in the carboxylate anion.<sup>17</sup> A similar value (1.27 Å) was found in 4(5)-carbamoylimidazolium-5(4)olate and in bredinin **1**.<sup>6</sup> The C(4)–C(6) bond (1.402(2) Å) is shorter than those reported for a C<sub>sp</sub><sup>2</sup>–C<sub>sp</sub><sup>1</sup> bond (1.430 Å) while the C≡N bond is, as in compound **5**, in the normal range of values, confirming the small demand of charge suggested by the NMR data.<sup>16</sup> All the previously reported values agree with two resonance chains, one localized on the O(8)–C(5)–C(4)–C(6) atoms (negative part of the molecule) and the other on the N(1)–C(2)–N(3) atoms (positive part of the molecule). The molecule is planar with a mean deviation from the plane of 0.011 Å; this planarity suggests an sp<sup>2</sup> hybridization of the N(1)<sup>δ+</sup> and N(3)<sup>δ+</sup> atoms.

Compound **3** crystallizes in a noncentrosymmetric and polar space group and, accordingly, a second harmonic

(16) Abbotto, A.; Bradamante, S.; Pagani, G. *J. Org. Chem.* **1993**, *58*, 449.

(17) Allen, F. H.; Kennard, O.; Watson, D. G.; Brammer, L.; Orpen, A. G.; Taylor, R. *J. Chem. Soc., Perkin Trans. 2*, **1987**, S1.

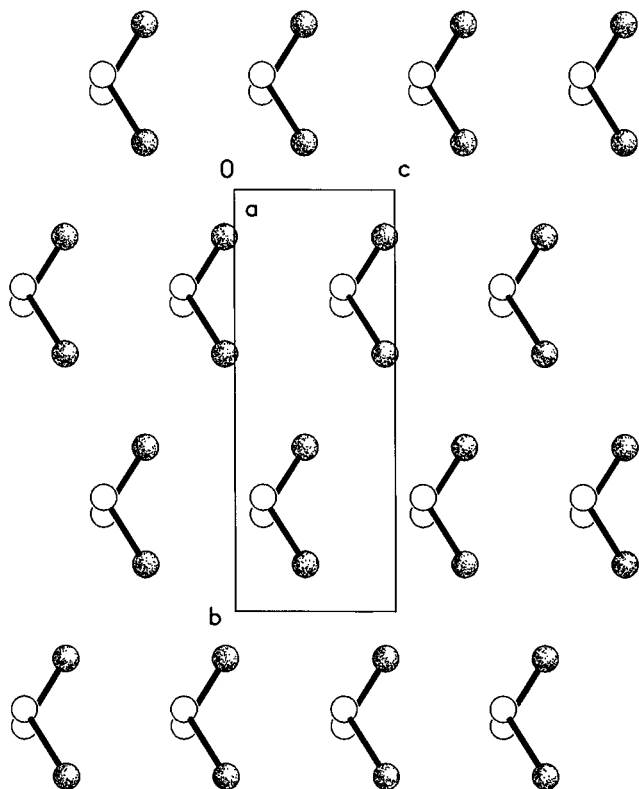


**Figure 3.** Figure showing the orientation of the molecular dipoles of compound **3** in the unit cell, where the white and the black circles correspond nearly to the barycenters of the positive and negative part of the molecules.

was generated by interaction of a laser beam at  $1.06 \mu\text{m}$  with a powder sample, following the experimental procedures of Kurtz and Perry.<sup>18</sup> Its efficiency appeared comparable to the efficiency of urea, a classical standard in this kind of measurements, and is correlated with its mesoionic character. If the molecules of compound **3** are sketched as dipoles, their preferential orientation along the polar  $c$  axis is apparent (Figure 3). The positive part of the molecule (NH, CH groups) acts as H-donor to the negative part of adjacent molecules (CO, CN groups).

**Molecular Structure of 4,4-Diphenyl-5-imidazolone (4) ( $\text{C}_{15}\text{H}_{12}\text{N}_2\text{O}$ ).** This compound crystallizes as colorless needles in the orthorhombic  $Pca2_1$  space group with  $a = 9.913(4) \text{ \AA}$ ,  $b = 15.181(5) \text{ \AA}$ ,  $c = 8.038(2) \text{ \AA}$ ,  $V = 1212.2(6) \text{ \AA}^3$ ,  $Z = 4$ ,  $D_c = 1.295 \text{ g cm}^{-3}$ ,  $W = 236.3$ ,  $R = 0.032$  for 1681 unique observed reflections with  $F > 4.0\sigma(F)$ ,  $\text{GOF} = 0.96$ . Figure 4 shows the view of the molecular structure of compound **4**. From the data in Table 2 for the four C–N bonds of the ring, a greater differentiation of values with respect to compound **3** is evident, in accord with the quite different pattern due to the absence of one of the two double bonds. In fact a double bond ( $1.269(3) \text{ \AA}$ ) is more localized between C(2) and N(3), while the N(1)–C(2) and N(1)–C(5) pairs ( $\text{C}_{\text{sp}^2}\text{--N}_{\text{sp}^3}$ ) and the N(3)–C(4) ( $\text{C}_{\text{sp}^3}\text{--N}_{\text{sp}^2}$ ) bond have a higher percentage of single bond character. The C(4)–C(5) distance corresponds to a single bond. The C(5)–O(6) bond length ( $1.218(3) \text{ \AA}$ ) is close to a ketonic carbonyl value. Including also O(6) and H atoms, the imidazole ring is planar; the mean deviation from the least-squares plane is  $0.027 \text{ \AA}$ . The phenyl rings are almost mutually perpendicular.

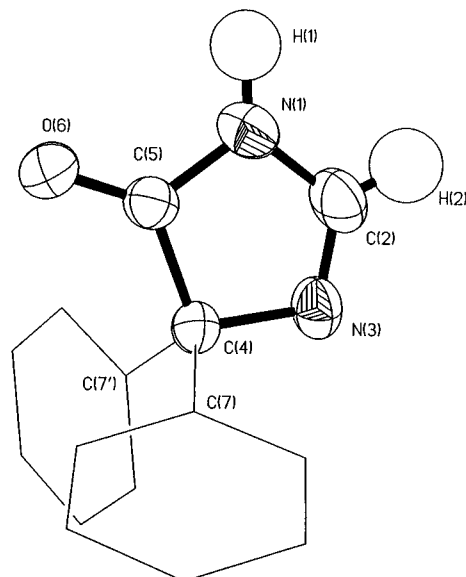


**Figure 4.** ORTEP plot (50% probability) of compound **4**.

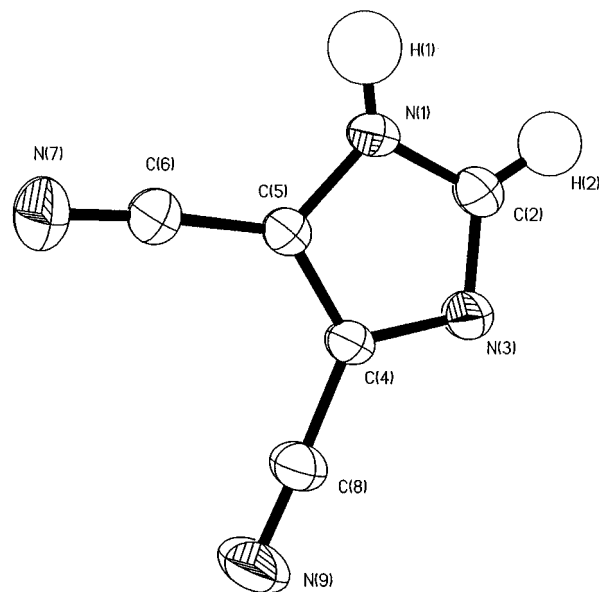


**Figure 5.** ORTEP plot (50% probability) of compound **5**.

The SHG is in keeping with the noncentrosymmetric space group  $Pca2_1$ . The efficiency of the SHG signal appeared 3 times smaller than the compound **3** efficiency, in agreement with the smaller polarization of compound **4**.

**Molecular Structure of 4,5-Dicyanoimidazole (5) ( $\text{C}_5\text{H}_2\text{N}_4$ ).** This compound crystallizes as colorless prisms in the monoclinic  $P2_1/c$  space group with  $a = 10.102(2) \text{ \AA}$ ,  $b = 7.528(2) \text{ \AA}$ ,  $c = 7.2520(10) \text{ \AA}$ ,  $\beta = 102.720(1)^\circ$ ,  $V = 538.0(2) \text{ \AA}^3$ ,  $Z = 4$ ,  $D_c = 1.458 \text{ g cm}^{-3}$ ,  $W = 118.1$ ,  $R = 0.041$  for 1249 unique observed reflections with  $F > 4.0\sigma(F)$ ,  $\text{GOF} = 0.91$ . Figure 5 shows the diagram of a molecule of compound **5**. This molecule shows the smallest range of C–N distances, determined by the presence of two double bonds in the imidazole ring (see Table 2). In fact, the bond range is  $1.318\text{--}1.396 \text{ \AA}$  for compound **3**,  $1.269\text{--}1.479 \text{ \AA}$  for compound **4**, and  $1.320\text{--}1.368 \text{ \AA}$  for compound **5**. The two C(4)–C(8) and C(5)–C(6) bond distances are slightly shorter than those reported for corresponding  $\text{C}_{\text{sp}^2}\text{--C}_{\text{sp}^1}$  distances,<sup>17</sup> thus suggesting a delocalization in the ring involving also

(18) Kurtz, S. K.; Perry, T. T. *J. Appl. Phys.* **1968**, *39*, 3798.

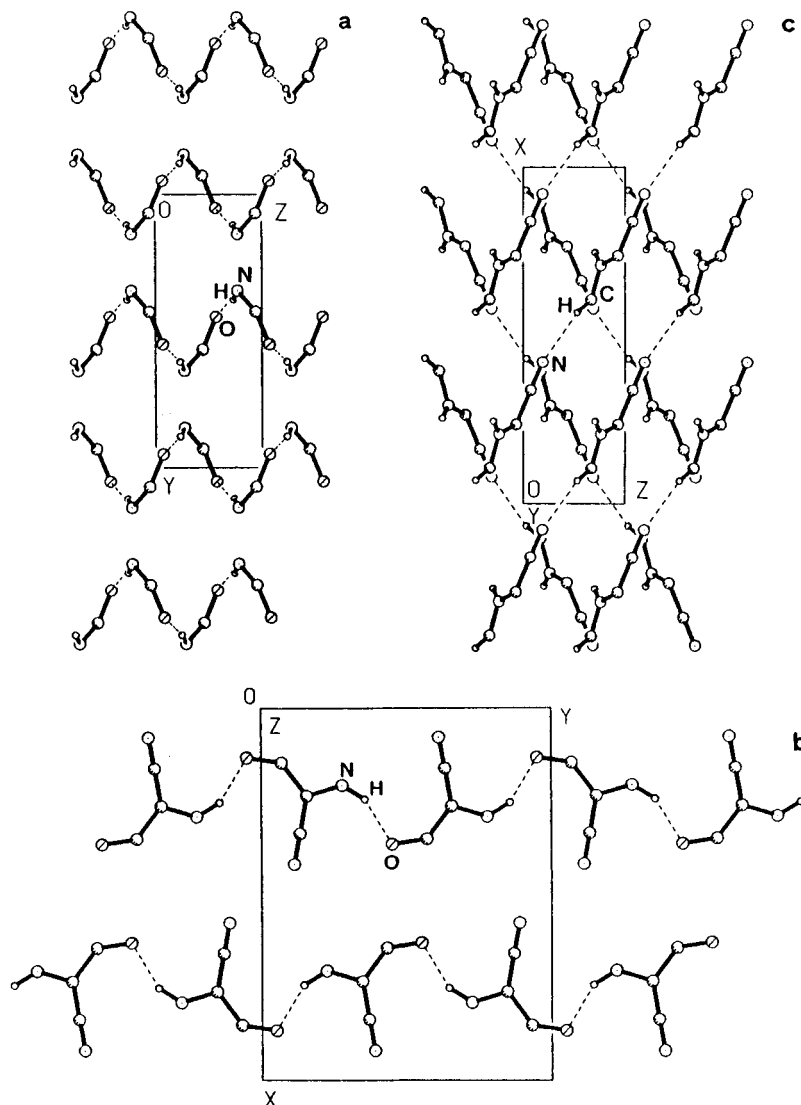


**Figure 6.** Plot of the HB's motifs for compound **3**: (a)  $C(4)$  motif of the  $O(8)\cdots H(1)-N(1)$  bond, (b)  $C(5)$  motif for the  $O(8)\cdots H(3)-N(3)$  hydrogen bonds, and (c)  $C(6)$  motif for the  $N(7)\cdots H(2)-C(2)$  hydrogen bonds. Some atoms are omitted for clarity.

these two bonds. The  $C\equiv N$  distances are in the normal range of values (see compound **3**). Obviously no SHG was detected.

**The Intermolecular Hydrogen Bonds.** An analysis of the HB's was made according to the encoding suggested by Etter.<sup>19</sup> For motifs generated from intermolecular HB's the designators are  $C_d^a$  (chain),  $R_d^a$  (ring), and  $D_d^a$  (dimer), where  $d$  and  $a$  are the number of donor and acceptors respectively in each motif; the size of the motif is shown in parentheses.

The types of HB's are:  $N-H\cdots O$  and  $C-H\cdots N\equiv C$  in compound **3**,  $N-H\cdots O$  and  $C-H\cdots O$  in compound **4** and  $N-H\cdots N\equiv C$  in compound **5**. The contacts are within 2.62 Å for the  $H\cdots O$  and  $H\cdots N$  distances.

**Compound 3.** The CO group acts as acceptor toward  $N(1)-H(1)$  and  $N(3)-H(3)$ , forming a three-center bond. The CN group acts as acceptor toward  $C(2)-H(2)$  in a quite rare arrangement. Consequently each molecule is involved in six HB's. In Table 4 the first HB gives a  $C(4)$  motif winding around the  $z_1$  axis (Figure 6a); the second HB has a  $C(5)$  wave motif (Figure 6b) and the third motif is a  $C(6)$  chain (Figure 6c), both showing a

**Table 4. Relevant Hydrogen Bonds Parameters**

compound <b>3</b>	N-H	H $\cdots$ O	N $\cdots$ O	N-H $\cdots$ O	C-O $\cdots$ H
$O(8)\cdots H(1)-N(1)$	0.91(2)	1.89(2)	2.785(2)	170(3)	123.1(7)
$O(8)\cdots H(3)-N(3)$	0.93(2)	1.85(2)	2.709(2)	154(2)	116.2(7)
	C-H	H $\cdots$ N	C $\cdots$ N	C-H $\cdots$ N	C-N $\cdots$ H
$N(7)\cdots H(2)-C(2)$	0.99(2)	2.30(3)	3.167(2)	145(2)	155.6(5)
compound <b>4</b>	N-H	H $\cdots$ O	N $\cdots$ O	N-H $\cdots$ O	C-O $\cdots$ H
$O(6)\cdots H(1)-N(1)$	0.95(3)	1.97(3)	2.914(3)	173(2)	137.7(7)
	C-H	H $\cdots$ O	C $\cdots$ O	C-H $\cdots$ O	C-O $\cdots$ H
$O(6)\cdots H(12)-C(12)$	0.96(0)	2.445(3)	3.333(3)	153.7(1)	115.5(2)
compound <b>5</b>	N-H	H $\cdots$ N	N $\cdots$ N	N-H $\cdots$ N	$C\equiv N\cdots$ H
$N(7)\cdots H(1)-N(1)$	0.90(2)	2.27(2)	3.048(1)	145(2)	173.3(5)
$N(9)\cdots H(1)-N(1)$	0.90(2)	2.28(2)	2.917(2)	127(1)	159.4(4)

reticulate in a view along the  $x$  and  $y$  directions, respectively. These three motifs intersect, giving rise to large rings involving five molecules with a  $R_5^4(18)$  graph. The presence of hydrogen bonds all around the molecule, as found in 2-amino-dicyanoimidazole,<sup>20</sup> justifies the IR absorptions, the nonmelting (only decomposition at 297–305 °C), and the low solubility in organic solvents and cold water.

(19) Etter, M. C. *Acc. Chem. Res.* **1990**, *23*, 120. Etter, M. C. *J. Phys. Chem.* **1991**, *95*, 4601.

(20) Hardgrove, J. Jr. *Acta Crystallogr. C* **1991**, *47*, 337.

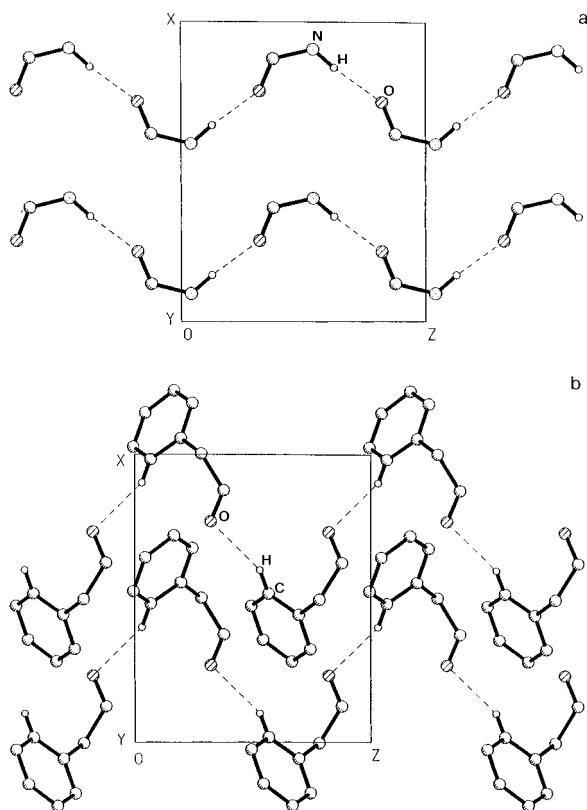


**Figure 7.** Plot of the HB's motifs for compound **4**: (a)  $C(4)$  motif for the  $O(6)\cdots H(1)-N(1)$  hydrogen bonds and (b)  $C(6)$  motif for the  $O(6)\cdots H(12)-C(12)$  hydrogen bonds. Only the moieties involved in the bonds are shown.

**Compound 4.** The  $N(1)-H(1)\cdots O(6)$  HB forms  $C(4)$  chains (Figure 7a) among the molecules related by the  $c$  planes. The second motif involves again  $O(6)$ , which acts as an acceptor toward  $H(12)-C(12)$  according to a  $C(6)$  graph (Figure 7b). The geometric parameters are summarized in Table 4.

Both chains intersect, forming two adjacent asymmetric rings  $R_2^2(10)$  that share the  $C(5)-O(6)$  bond. The  $O\cdots H-N$  HB's values in compounds **3** and **4** are fully in accordance with the values reported in ref 21.

**Compound 5.** The CO group is absent in this compound and only the nitrile substituents are the HB acceptors toward the  $N-H$  donors with formation of  $N\cdots H-N$  bonds. The three molecules involved in the HB's generate  $R_2^3(12)$  graphs. These rings are planar, adjacent, and share three edges, forming therefore ribbons lying along the  $y$  axis (Figure 8). The geometric parameters of these contacts are listed in Table 4. The  $N\cdots N$  distances are within the range found in crystals containing  $=N-H\cdots N$  and  $NH_2\cdots N$  HB's.<sup>22</sup>

The three crystal structures studied show three types of H-acceptors (CN, =O, and =N) and two types of H-donors ( $=NH$  and  $=CH$  moieties belonging to the imidazole or to a phenyl ring). Intramolecular HB's are not possible, except for compound **4**, where there is a weak contact (2.62 Å) between  $O(6)$  and  $H(8')$ . The  $N(3)$  atom does not act as an acceptor, as, for example, in imidazole,<sup>23</sup> except for in compound **3**, while the NH

group is always an H-donor. In compounds **4** and **5** the  $N(3)$  atom becomes an H-acceptor when the range of the considered distances is expanded. In this case the H-donor is a CH group. In compound **4** the CH group belongs to a phenyl moiety ( $C(12')-H(12')\cdots N(3)$  2.711 Å,  $N(3)\cdots C(12')$  3.557 Å,  $N(3)\cdots H(12')-C(12')$  150.3°, with the CH group lying on the plane of the imidazole ring). In compound **5**, the CH group is part of the imidazole ring ( $C(2)-H(2)\cdots N(3)$  2.636 Å,  $C(2)\cdots N(3)$  3.582 Å,  $C(2)-H(2)\cdots N(3)$  165°), and it creates the connection among the ribbons shown in Figure 8. The  $C\equiv N$  group acts as an H-acceptor in competition with  $N(3)$ , suggesting that the rank as H-acceptor of CN is greater than for  $=N$  in the compounds studied. A feature common to **3** and **4** is due to the behavior of  $=O$  as acceptor toward two H-donors; in compound **3** the two best donors are the  $=NH$  groups, while in compound **4** only one NH is present and the second bond is made consequently with an aromatic CH.

## Conclusions

The present study on imidazole derivatives showed the mesoionic character of compound **3**. The hydrogen bonding was also examined: (i) unusual  $C-H\cdots N\equiv C$  and  $C-H\cdots O$  bonds for the 4-cyanoimidazolium-5-olate and 4,4-diphenyl-5-imidazolinone respectively, and (ii) formation of six hydrogen bonds for **3**, justifying the lack of a defined melting point, the high degradation temperature, the insolubility in organic solvent, and the IR properties. Nonlinear optical properties were also demonstrated. The efficiency of the second harmonic generation, the high thermal stability, the easy and economic synthesis and the transparency in visible region make the 4-cyanoimidazolium-5-olate an interesting candidate for nonlinear optics as single crystal.

## Experimental Section

**4-Cyanoimidazolium-5-olate (3).** Compound **3** was prepared according to the literature procedure. Mp: 297–305 °C (dec) (DSC) (lit.<sup>10</sup> mp: 360 °C (dec)). UV–vis in EtOH (95%)  $\lambda_{\max}$ , nm (log  $\epsilon$ ): 232 (3.77), 262 (3.66). <sup>1</sup>H NMR (400 MHz, DMSO- $d_6$ )  $\delta$  (ppm): 7.70 (s, 1H), 11.82 (s, 2H). <sup>13</sup>C NMR (100 MHz, DMSO- $d_6$ )  $\delta$  (ppm): 159.62, 131.52 (<sup>1</sup> $J_{CH} = 214$  Hz), 115.05, 80.60. Anal. Calcd for  $C_4H_3N_3O_1$ : C, 44.04; H, 2.77; N, 38.52; O, 14.67. Found: C, 43.97; H, 2.78; N, 38.57; O, 14.64.

**4,4-Diphenyl-4H-imidazol-5-one (4).** Compound **4** was prepared according to the literature procedure mp: 168 °C (lit.<sup>24</sup> mp: 166–167 °C). UV–vis in EtOH (95%)  $\lambda_{\max} = 205$  nm, log  $\epsilon = 4.54$ . <sup>1</sup>H NMR (400 MHz, DMSO- $d_6$ )  $\delta$  (ppm): 7.33 (m, 10H), 8.27 (s, 1H), 11.0 (br s, 1H). <sup>13</sup>C NMR (100 MHz, DMSO- $d_6$ )  $\delta$  (ppm): 76.00 (br s, 1C), 126.88 (4C, Ph), 127.59 (2C, Ph), 128.43 (4C, Ph), 140.27 (2C, Ph), 153.14 (br s, 1C), 183.71 (br s, 1C, CO). Anal. Calcd for  $C_{15}H_{12}N_2O_1$ : C, 76.25; H, 5.12; N, 11.86; O, 6.77. Found: C, 76.10; H, 5.10; N, 11.88; O, 6.78.

**4,5-Dicyanoimidazole (5).** Compound **5**, available commercially, was purified further by crystallization from ethyl acetate. mp: 175 °C (lit.<sup>25</sup> mp: 175 °C). UV–vis in EtOH (95%) ( $\lambda_{\max} = 246$  nm, log  $\epsilon = 4.09$ ). <sup>1</sup>H NMR (400 MHz, DMSO- $d_6$ )  $\delta$  (ppm): 8.16 (s, 1H), 13.55 (br s, 1H). <sup>13</sup>C NMR (100 MHz, DMSO- $d_6$ )  $\delta$  (ppm): 111.20 (s, 2C), 115.40 (s, 2C, CN), 141.74 (d, <sup>1</sup> $J_{CH} = 217$ , 1C). Anal. Calcd for  $C_3H_2N_2O_1$ : C, 76.25; H, 5.12; N, 11.86; O, 6.77. Found: C, 76.10; H, 5.14; N, 11.82; O, 6.75.

**X-ray Analysis.**<sup>28</sup> Single crystals of compound **3** were obtained by dissolving 50 mg of product in 4 mL of boiling water in a screw-top sealed vial. Slow cooling was performed by immersion in a programmable bath, whose temperature was set

(21) Taylor, R.; Kennard, O.; Versichel, W. *Acta Crystallogr. B* **1984**, *40*, 280.

(22) Gavezzotti, A.; Filippini, G. *J. Phys. Chem.* **1994**, *98*, 4831.

(23) Craven, B. M.; Mc Mullan, R. K.; Bell, J. D.; Freeman, H. C. *Acta Crystallogr. B* **1977**, *33*, 2585.

(24) Biltz, H.; Seydel, K. *Ann. Chem.* **1912**, *391*, 215.

(25) Woodward, D. W. U.S. Patent 2, 534, 331/1950 (*Chem. Abstr.* **45**, 5191d).

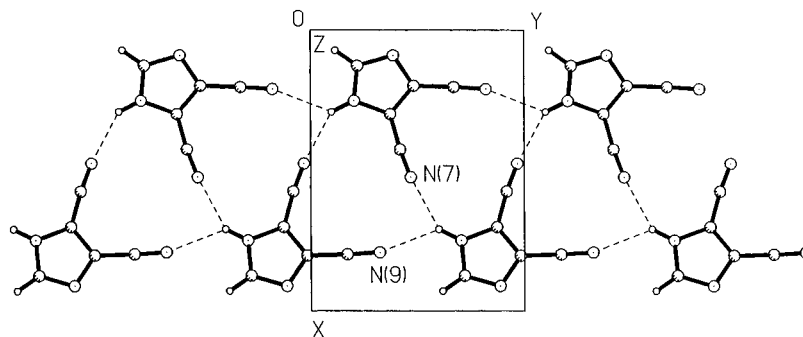


**Figure 8.** Plot of the  $R_2^3$  (12) motif for the  $\text{C}\equiv\text{N}(7,9)\cdots\text{H}(1)\text{--N}(1)$  hydrogen bonds of compound **5**.

to achieve room temperature in 1 week. Single crystals of compounds **4** and **5** were obtained in a similar manner by dissolving the samples (150 mg of compound **4** and 200 mg of compound **5**) in 10 mL of ethyl acetate using an open vial and by slow evaporation of the solvent at room temperature.

X-ray data were collected on an automatic diffractometer at room temperature, using graphite-monochromated Mo  $K\alpha$  radiation ( $\lambda = 0.71073 \text{ \AA}$ ). A total of 26 independent reflections with  $20^\circ < 2\theta < 30^\circ$  were used for least squares determinations of cell constants. Intensities of two reflections were monitored every 50 measurements and indicated no decomposition. The three structures were solved by direct methods using SIR92<sup>26</sup> and refined (on  $\sum w(F_o - F_c)^2$ ) by full-matrix least-squares. Nonhydrogen atoms were refined with anisotropic thermal parameters. The position of H atoms was localized in the final Fourier-difference maps and was refined with an isotropic thermal factor; the H atoms of phenyl groups in compound **4** were refined riding on corresponding C atoms with fixed  $U_{\text{iso}}$ . At convergence all shifts were  $<0.11\sigma$  (compound **3**),  $<0.002\sigma$  (compound **4**) and  $<0.05\sigma$  (compound **5**). The largest peak and hole in final difference map were 0.20 and  $-0.21 \text{ e \AA}^{-3}$  for **3**, 0.20 and  $-0.32 \text{ e \AA}^{-3}$  for **4**, and 0.30 and  $-0.25 \text{ e \AA}^{-3}$  for **5**. Data reduction and application of corrections for absorption (empirical correction using the method reported by North et al.<sup>27</sup>), refine-

ments, and all other calculation and figure were performed using the program SHELXTL PLUS (PC version).

**Acknowledgment.** This work was supported by the C. N. R. and M. U. R. S. T. (Italy). The authors thank Dr. Joseph Zyss of the Laboratoire de Bagnoux of the Centre National d'Etudes des Télécommunications of France Telecom for the SHG measurements.

**Supporting Information Available:**  $^{13}\text{C}$  NMR spectra of the solid state and DMSO- $d_6$  solution of compound **3**, full lists of infrared, mass spectral fragmentations of compounds **3–5**, bond angles and lengths of benzene rings of compound **4**; crystal data, refinement parameters, atomic fractional coordinates, and anisotropic thermal parameters for compounds **3–5** (20 pages). This material is contained in libraries on microfiche, immediately follows this article in the microfilm version of the journal, and can be ordered from the ACS; see any current masthead page for ordering information.

JO9621480

(26) Altomare, A.; Cascarano, G.; Giacovazzo, C.; Guagliardi, A.; Burla, M. C.; Polidori, G.; Camalli, M. *J. Appl. Crystallogr.* **1994**, *27*, 435.

(27) North, A. C.; Phillips, D. C.; Mathews, F. S. *Acta Crystallogr., Sect. A* **1968**, *24*, 351.

(28) The authors have deposited atomic coordinates for the structures depicted in Figures 2, 4, and 5 with the Cambridge Crystallographic Data Centre. The coordinates can be obtained, upon request, from the Director, Cambridge Crystallographic Data Centre, 12 Union Road, Cambridge, CB2 1EZ, UK.